*Research Article*

# Enhanced Photodecomposition of Methylene Blue in Water with $Sr_{1-x}K_xTiO_{3-\delta}$@PC-polyHIPEs under UV and Visible Light

**Yonghua Gao** (ID),[1,2] **Tao Zhang,**[2] **Qipeng Guo,**[2] **and Lizhen Gao** (ID)[1]

[1]*School of Environmental Science and Engineering, Taiyuan University of Technology, Taiyuan 030024, China*
[2]*Polymers Research Group, Institute for Frontier Materials, Deakin University, Locked Bag 20000, Geelong, VIC 3220, Australia*

Correspondence should be addressed to Lizhen Gao; gaolizhen@tyut.edu.cn

Photocatalytic method was investigated to remove water pollutant methylene blue (MB) produced in textile, plastic, and dye industries. PC-polyHIPEs were prepared by light-induced polymerization of dopamine in transparent polyHIPEs which were synthesized by polymerization within high internal phase emulsions. $Sr_{1-x}K_xTiO_{3-\delta}$ ($x = 0$–$0.5$) nanoparticles were incorporated and adhered to PC-polyHIPEs to form $Sr_{1-x}K_xTiO_{3-\delta}$@PC-polyHIPEs for the first time. The catalysts were characterized by XRD, FTIR, TGA, UV-Vis DRS, and SEM and their photocatalytic properties for MB decomposition were measured over UV-Vis spectrometer. The PC-polyHIPEs were of interconnected porous structure with around $100\,\mu m$ pores and $30\,\mu m$ windows. $Sr_{1-x}K_xTiO_{3-\delta}$@PC-polyHIPEs showed excellent MB decomposition activity under either UV or visible light although $Sr_{1-x}K_xTiO_{3-\delta}$ alone worked only under UV light. When $x = 0.3$, $Sr_{1-x}K_xTiO_{3-\delta}$@PC-polyHIPEs showed the highest photocatalytic performance due to the existence of more oxygen vacancies. When the water solution with $50\,mg\,L^{-1}$ MB and $1.6\,g_{cat.}\,L^{-1}$ $Sr_{0.7}K_{0.3}TiO_{3-\delta}$@PC-polyHIPEs was exposed to visible light for 160 min at room temperature, 88.3% of MB was decomposed. After being used for eight cycles, 87.6% activity of fresh $Sr_{0.7}K_{0.3}TiO_{3-\delta}$@PC-polyHIPEs still remained. The influences of salinity, temperature, and catalyst concentration on the catalytic activity were studied. For MB decomposition under visible light, the activation energy of $Sr_{0.7}K_{0.3}TiO_{3-\delta}$@PC-polyHIPEs was calculated to be $12.3\,kJ\,mol^{-1}$ and the kinetics analysis revealed that the photocatalysis followed the second-order reaction. These findings demonstrated that $Sr_{1-x}K_xTiO_{3-\delta}$@PC-polyHIPEs were an effective candidate for real application in decomposition of MB in water.

## 1. Introduction

Methylene blue (MB) dye is produced as a water pollutant from textiles, cosmetics, printing, dyeing, food processing, and paper-making industries [1, 2]. Discharge of this colored effluent presents a major environmental problem for developing countries because of its toxic and carcinogenic effects on living beings [1]. There are several technologies adopted to remove MB in water like biological degradation, adsorption, Fenton's reagent method, coagulation processes, photocatalytic decomposition, and so on [3]. Among these, photocatalytic method to degrade these pollutants is the most desirable as no second pollutants are generated in this process [4]. $SrTiO_3$ has been an attractive catalyst for organics degradation under UV light [5–8]. However, there are some disadvantages hindering its real application, such as

easy precipitation and agglomeration [9], low photocatalytic efficiency under visible light [10–12], and the difficulty of collection and separation [13]. To overcome such disadvantages, incorporation of $SrTiO_3$ into a catalyst support and substitution of potassium ion ($K^+$) for part of $Sr^{2+}$ in $SrTiO_3$ to generate oxygen vacancy ($Sr_{1-x}K_xTiO_{3-\delta}$) may favour the improvement of its photocatalytic activity.

Up to now, different kinds of inorganic porous catalyst supports have been reported [14], but little porous polymer catalyst support has been used. Compared to inorganic supports, polymer owns the following advantages and is more suitable for water treatment: low density, big pores, inertia to acids and bases, flexibility, low cost, and high viscosity [15–18]. Polydopamine coated polyHIPEs (PC-polyHIPEs) are a type of macroporous polymer, which has been confirmed to be an excellent catalyst support and has large

attachment to inorganic catalyst particles. It is synthesized by light inducing polymerization of dopamine in transparent polyHIPEs obtained via polymerization within high internal phase emulsions (HIPEs) [19–23]. The transparent substrate and macropores facilitate the adsorption of light, the mass transfer of substances like gases or liquids, and the host-guest interactions [24].

In this paper, with incorporation of $Sr_{1-x}K_xTiO_{3-\delta}$ nanoparticles into PC-polyHIPEs, we obtained an efficient and durable material for photodecomposition of MB in model wastewater under visible light.

## 2. Experimental

*2.1. Materials.* Chemicals $Ti(OBu)_4$, $Sr(NO_3)_2 \cdot 6H_2O$, $KNO_3$, ethanol, ethylene glycol, anhydrous acetic acid, butyl acrylate, ethylene glycol dimethacrylate, sulfonated polystyrene, 2-hydroxy-2-methylpropiophenone, dopamine, and glycerol were purchased from Sigma-Aldrich.

*2.2. Preparation of PC-polyHIPEs.* PC-polyHIPEs were prepared according to the method described in our previous paper [22]. In a word, it was obtained by light inducing polymerization of dopamine in transparent polyHIPEs which was made via polymerization within high internal phase emulsions.

*2.3. Preparation of $Sr_{1-x}K_xTiO_{3-\delta}$ Nanoparticles.* $Sr_{1-x}K_xTiO_{3-\delta}$ nanoparticles were prepared by means of sol-gel. Typically, 1 mL of $Ti(OBu)_4$ was mixed with 3 mL of ethanol and 0.3 mL of anhydrous acetic acid to form a titanium precursor solution. $Sr(NO_3)_2$ and $KNO_3$ aqueous solution (1 M) were added dropwise to the as-prepared titanium precursor solution with the expected stoichiometry at room temperature. The resulting solution was stirred to turn into milky sol and finally transformed to gel. Afterwards, the wet gel was dried at 120°C overnight, and then the foamy solid was heated to 200°C in air in a tube furnace at a rate of 5°C min$^{-1}$ to remove the organic ligands. Successively, the precursor was heated to 450°C and kept for 3 h to decompose the nitrates and calcined at 850°C for 4 h in air. Finally, it was ground to obtain $Sr_{1-x}K_xTiO_{3-\delta}$ nanoparticles.

*2.4. Preparation of $Sr_{1-x}K_xTiO_{3-\delta}$@PC-polyHIPEs.* The photocatalyst $Sr_{1-x}K_xTiO_{3-\delta}$@PC-polyHIPEs was fabricated by chemical impregnation method [25]. In short, 100 mg of $Sr_{1-x}K_xTiO_{3-\delta}$ nanoparticles was dispersed into 500 mL of mixed solvents (ethylene glycol : ethanol = 7 : 3, V/V) under sonication for 1 h, and then 80 mg of PC-polyHIPEs was immersed into the as-obtained solution. After 24 h, the as-formed $Sr_{1-x}K_xTiO_{3-\delta}$@PC-polyHIPEs were collected and washed repeatedly followed by drying at 110°C for 12 h. The dried $Sr_{1-x}K_xTiO_{3-\delta}$@PC-polyHIPEs were then centrifuged in water with 7000 rpm to make sure that only the stabilized imbedded $Sr_{1-x}K_xTiO_{3-\delta}$ remained onto the PC-polyHIPEs.

*2.5. Characterization.* X-ray diffraction test was recorded on X'pert Powder diffractometer (XRD, PANalytical Company, Holland), using Cu $K\alpha$ ($\lambda$ = 0.1541 nm) radiation at 40 kV

and 30 mA with a step scan of 0.065°. The Fourier transform infrared (FTIR) spectra were carried out on a Bruker Vertex 70 FTIR spectrometer from 4000 to 600 cm$^{-1}$ with a resolution of 4 cm$^{-1}$. The morphologies were observed with scanning electron microscopy (SEM, JSM-7800F, JEOL) at 3 kV. The Brunauer-Emmett-Teller (BET) specific surface area, pore volume, and pore width were operated on BET Tristar 3000 analyzer (Micromeritics, United States). TGA analyzer (Q50, TA instrument) was used to measure the weight loss and differential TG curves of the samples. Each time, about 5 mg of the sample was loaded in the platinum crucible and heated in air from room temperature to 800°C at a heating rate of 10°C min$^{-1}$. The UV-Vis diffuse reflection spectroscopy (UV-Vis DRS) of samples was measured with a UV-Visible system (Agilent Varian Cary 100) equipped with a labsphere diffuse reflectance accessory.

*2.6. Photocatalytic Activity Evaluation.* The photocatalytic activities of $Sr_{1-x}K_xTiO_{3-\delta}$ nanoparticles and $Sr_{1-x}K_xTiO_{3-\delta}$@PC-polyHIPEs were evaluated by decomposition of MB. In each run, $Sr_{1-x}K_xTiO_{3-\delta}$ nanoparticles or $Sr_{1-x}K_xTiO_{3-\delta}$@PC-polyHIPEs were, respectively, dispersed into 100 mL MB aqueous solutions and then kept at dark for 2 h to establish the adsorption-desorption equilibrium. The initial concentration $C_0$ of MB was recorded after the equilibrium was established. Then all the experiments were conducted at room temperature with pH = 7 at various irradiation time under UV or visible light with an initial MB concentration of 50 mg L$^{-1}$. The photocatalytic process was made over a homemade light exposure system under UV at wavelength of 365 nm or visible light at 450 nm. The average light intensity is 3.0 mW cm$^{-2}$. The photocatalytic activity was obtained by measuring the concentration of MB solution recorded on a UV-Vis spectrometer (Cary 3 UV-Visible, Agilent, United States) at $\lambda$ = 664 nm. Before MB concentration measurement, for $Sr_{1-x}K_xTiO_{3-\delta}$@PC-polyHIPEs, the sponge-like catalyst was readily removed, while, for $Sr_{1-x}K_xTiO_{3-\delta}$ catalyst, the nanoparticle suspension solution was centrifuged at 7000 rpm for 30 min to precipitate the particles to make sure the measurement is accurate. The MB degradation efficiency ($\eta$%) can be calculated with the following:

$$\eta\% = \left(1 - \frac{C}{C_0}\right) \times 100. \qquad (1)$$

In the equation, $C_0$ and $C$ correspond to the initial concentration and the concentration of MB at time $t$, respectively. For comparison, the amount of $Sr_{1-x}K_xTiO_{3-\delta}$ was kept the same in $Sr_{1-x}K_xTiO_{3-\delta}$ and $Sr_{1-x}K_xTiO_{3-\delta}$@PC-polyHIPEs catalysts during the test (the loading concentration of $Sr_{1-x}K_xTiO_{3-\delta}$ would be confirmed by TGA).

## 3. Results and Discussion

*3.1. Characterization of $Sr_{1-x}K_xTiO_{3-\delta}$.* The XRD patterns of $Sr_{1-x}K_xTiO_{3-\delta}$ are presented in Figure 1. All the main diffraction peaks can be readily assigned to the cubic perovskite structure of $SrTiO_3$ (JCPDS 35-0734), demonstrating that the perovskite structure is still well maintained after K$^+$
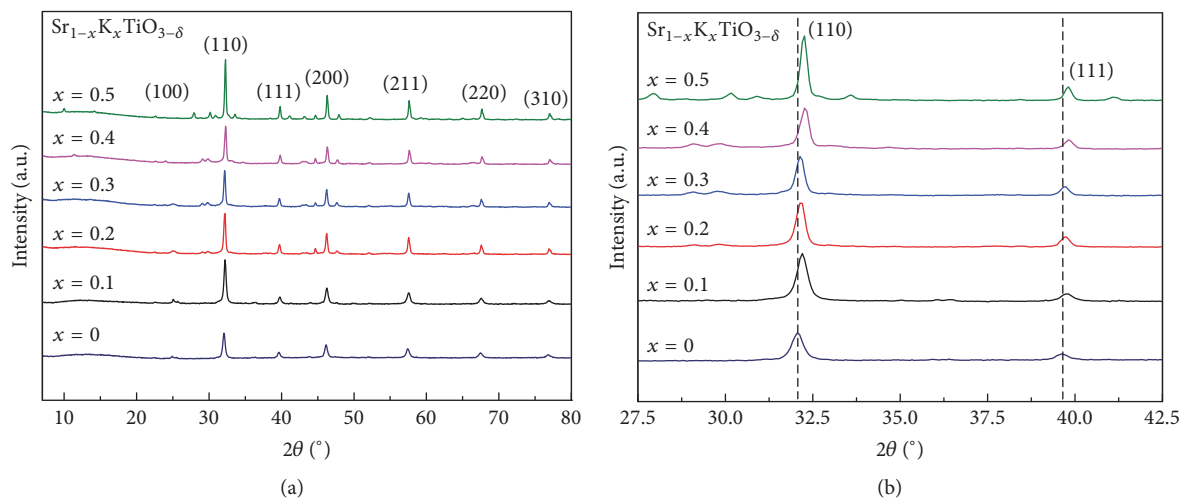
FIGURE 1: XRD patterns of the as-synthesized $Sr_{1-x}K_xTiO_{3-\delta}$.
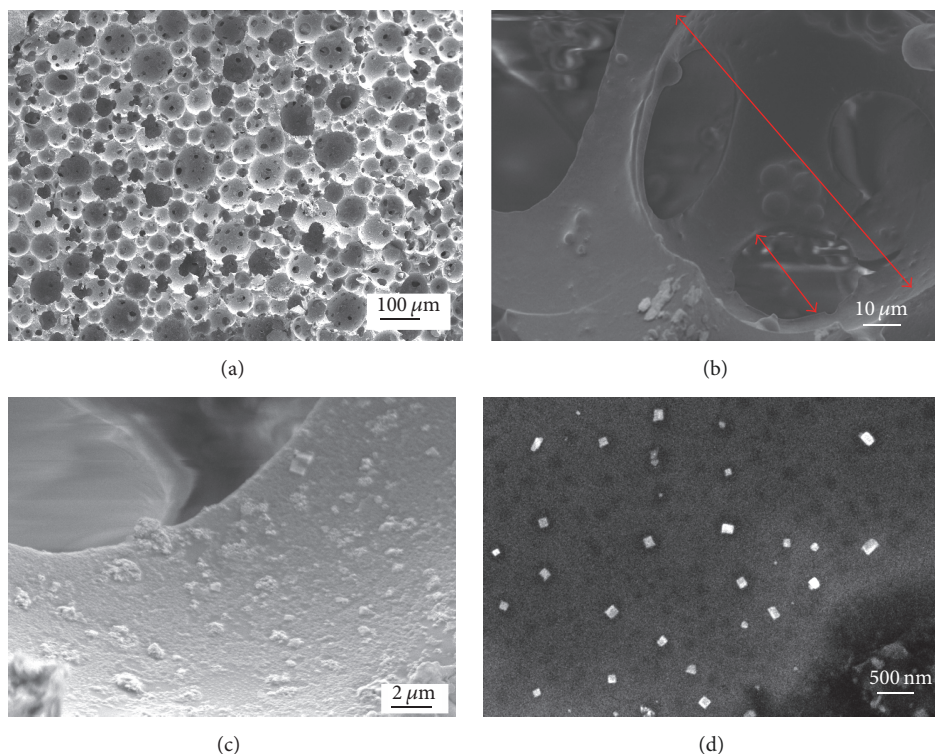


FIGURE 2: SEM micrographs of (a) PC-polyHIPEs; (b) enlarged PC-polyHIPEs; (c) $Sr_{0.7}K_{0.3}TiO_{3-\delta}$@PC-polyHIPEs; (d) $Sr_{0.7}K_{0.3}TiO_{3-\delta}$. The long red arrow in Figure 2(b) shows that the PC-polyHIPEs own ca. 100 $\mu$m pores and the short red arrow shows that the PC-polyHIPEs own ca. 30 $\mu$m windows.

substitution. When $x \geq 0.3$, there are some weak diffraction peaks appearing at $2\theta = 30.23°$, 44.60°, and 47.63° which are corresponding to $TiO_2$ lattice diffraction. Furthermore, the perovskite structure diffraction peaks correspond to the lattice faces of (110), (111), (200), (211), (220), and (310) which turn to be much sharper (Figure 1(a)). The patterns shown in Figure 1(b) demonstrated that the lattice faces of

(110) and (111) turn to be higher $2\theta$ with increasing K-doping amount, suggesting that $d$ becomes smaller with the K-doping. Figure 2 illustrates SEM morphologies of PC-polyHIPEs, $Sr_{0.7}K_{0.3}TiO_{3-\delta}$, and $Sr_{0.7}K_{0.3}TiO_{3-\delta}$@PC-polyHIPEs. Figure 2(a) shows that PC-polyHIPEs has a well-developed interconnected macroporous structure, with smaller holes embedded in larger holes. It can be clearly
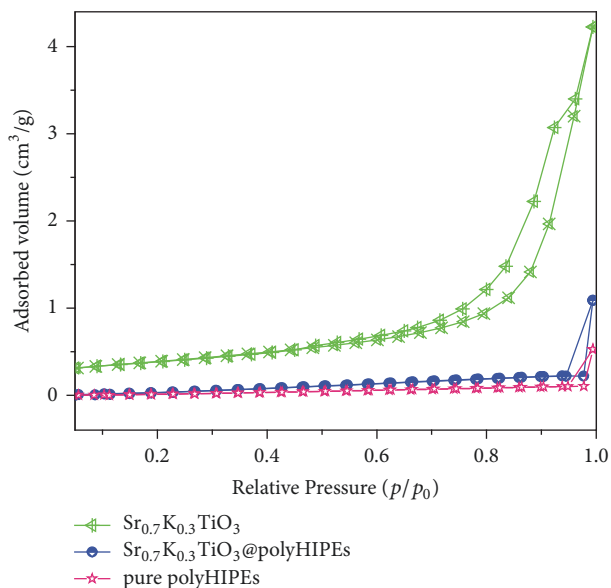
TABLE 1: Specific surface areas of $Sr_{1-x}K_xTiO_{3-\delta}$ samples.

| Catalysts | BET ($m^2/g$) | Pore volume ($cm^3/g$) | Average pore width (nm) |
|---|---|---|---|
| $SrTiO_3$ | 30.02 | 0.11 | 14.76 |
| $Sr_{0.9}K_{0.1}TiO_{3-\delta}$ | 30.08 | 0.12 | 16.59 |
| $Sr_{0.8}K_{0.2}TiO_{3-\delta}$ | 30.77 | 0.13 | 17.47 |
| $Sr_{0.7}K_{0.3}TiO_{3-\delta}$ | 31.09 | 0.15 | 20.89 |
| $Sr_{0.6}K_{0.4}TiO_{3-\delta}$ | 28.16 | 0.09 | 19.87 |
| $Sr_{0.5}K_{0.5}TiO_{3-\delta}$ | 25.24 | 0.08 | 19.31 |
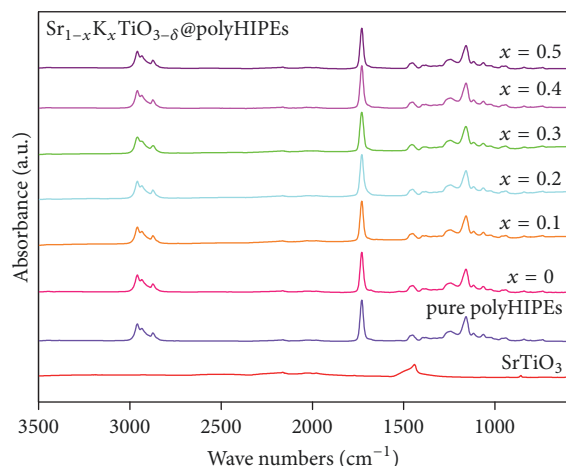


FIGURE 3: Ftir spectra of $Sr_{1-x}K_xTiO_{3-\delta}$@PC-polyHIPEs and PC-polyHIPEs.



FIGURE 4: $N_2$ adsorption-desorption isotherms of $Sr_{0.7}K_{0.3}TiO_{3-\delta}$, PC-polyHIPEs, and $Sr_{0.7}K_{0.3}TiO_{3-\delta}$@PC-polyHIPEs.

observed that the PC-polyHIPEs owns ca. 100 $\mu$m pores and 30 $\mu$m windows as shown in the magnified micrograph of PC-polyHIPEs in Figure 2(b). Such kind of stable regular large scaled porous structure of PC-polyHIPEs is hard to be obtained for inorganic catalyst supports. Figure 2(c) indicates that when $Sr_{0.7}K_{0.3}TiO_{3-\delta}$ nanoparticles are incorporated, the interconnected macroporous structure of PC-polyHIPEs is well preserved. The higher magnification micrograph demonstrated in Figure 2(d) confirms that well-defined cubic nanoparticles structure has been successfully incorporated into the PC-polyHIPEs. The average size of these cubic primary particles is 100 nm. However, some smaller nanoparticles with diameter about 10 nm coexist. Moreover, these nanoparticles are dispersed evenly without aggregation, which indicates $Sr_{0.7}K_{0.3}TiO_{3-\delta}$ has strongly adhered to PC-polyHIPEs. The strong adherence between PC-polyHIPEs and $Sr_{0.7}K_{0.3}TiO_{3-\delta}$ nanoparticles ensures the durability of catalyst when reacting with organic compounds in water. These results demonstrate that the high viscosity of PC-polyHIPEs plays an important role in producing an inorganic/polymer composite porous catalyst.

The formation of the hybrid $Sr_{1-x}K_xTiO_{3-\delta}$@PC-polyHIPEs catalyst is confirmed by FTIR. The spectra of $Sr_{1-x}K_xTiO_{3-\delta}$@PC-polyHIPEs, PC-polyHIPEs, and $SrTiO_3$ are displayed in Figure 3. Pure $SrTiO_3$ has an obvious peak at 1433 $cm^{-1}$. PC-polyHIPEs showed three distinct peaks at

2962, 1726, and 1159 $cm^{-1}$. Characteristic peaks appeared at 1433, 2962, 1726, and 1159 $cm^{-1}$ in $Sr_{1-x}K_xTiO_{3-\delta}$@PC-polyHIPEs, indicating that potassium is successfully incorporated into $SrTiO_3$ and is adhered to PC-polyHIPEs.

The BET specific surface areas (SSA) of the $Sr_{1-x}K_xTiO_{3-\delta}$ photocatalyst after K-doping are shown in Table 1. It can be seen that all the nanocatalysts $Sr_{1-x}K_xTiO_{3-\delta}$ have larger SSA after calcination at 850°C. With the increasing amount of K-doping, the SSA of $Sr_{1-x}K_xTiO_{3-\delta}$ gradually increases, and the nanocubic $Sr_{0.7}K_{0.3}TiO_{3-\delta}$ has the largest SSA of 31.09 $m^2\,g^{-1}$. However, when the amount of K substitution exceeds 30%, the SSA of the catalyst $Sr_{1-x}K_xTiO_{3-\delta}$ decreases gradually. The SSA of $Sr_{0.6}K_{0.4}TiO_{3-\delta}$ and $Sr_{0.5}K_{0.5}TiO_{3-\delta}$ is 28.16 and 25.24 $m^2\,g^{-1}$, respectively. When the doping amount is more than 30%, two phases of perovskite structure $Sr_{1-x}K_xTiO_{3-\delta}$ and $TiO_2$ are formed, which may cause the SSA to decrease.

Taking $Sr_{0.7}K_{0.3}TiO_{3-\delta}$ as an example, the $N_2$ adsorption-desorption curves of $Sr_{0.7}K_{0.3}TiO_{3-\delta}$ nanoparticles and $Sr_{0.7}K_{0.3}TiO_{3-\delta}$@PC-polyHIPEs are shown in Figure 4 after cooperating with the PC-polyHIPEs.

According to IUPAC classification, the $N_2$ adsorption-desorption curves of these three samples belong to the
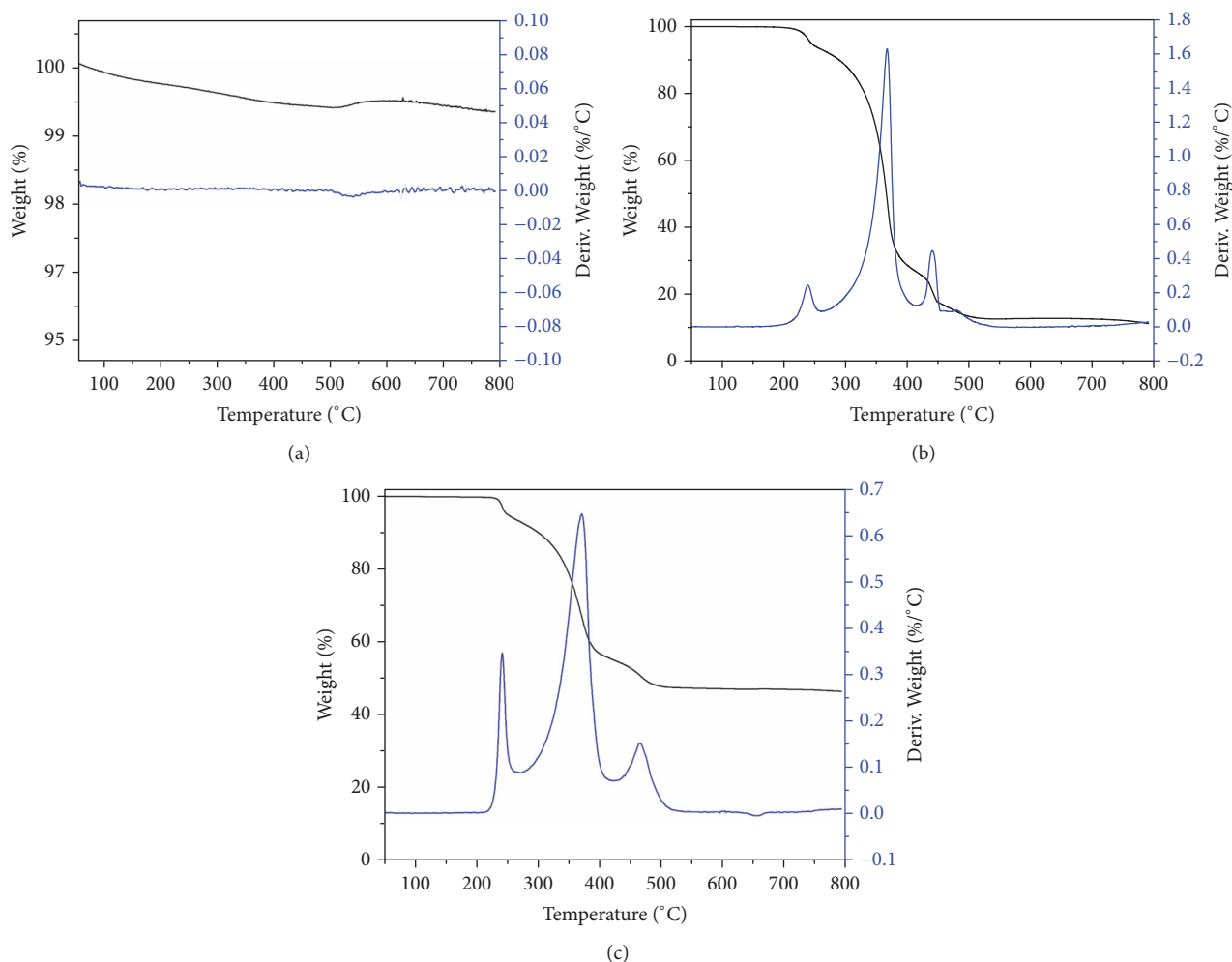
(a)

(b)

(c)

FIGURE 5: TG-DTG curves of (a) $Sr_{0.7}K_{0.3}TiO_{3-\delta}$; (b) PC-polyHIPEs; and (c) $Sr_{0.7}K_{0.3}TiO_{3-\delta}$@PC-polyHIPEs.

IV-type curve with hysteresis loop. The hysteresis loop of $Sr_{0.7}K_{0.3}TiO_{3-\delta}$ is located at 0.5~0.96 ($p/p_0$), indicating that there are micropores and mesopores in $Sr_{0.7}K_{0.3}TiO_{3-\delta}$. Based on this result, the average pore width of $Sr_{0.7}K_{0.3}TiO_{3-\delta}$ is 20.89 nm. And the hysteresis loop position ($p/p_0 = 0.96$) of the support PC-polyHIPEs and the composite material $Sr_{0.7}K_{0.3}TiO_{3-\delta}$@PC-polyHIPEs are almost the same, indicating that the samples are of macroporous structure [26]. As the pores in PC-polyHIPEs are 30~100 $\mu$m in diameter, over such material, the $N_2$ adsorption-desorption isothermal curve does not exactly reflect the pore situation. The SSA of the pure support PC-polyHIPEs is 0.113 $m^2 g^{-1}$. After adding $Sr_{0.7}K_{0.3}TiO_{3-\delta}$, the SSA of the composite $Sr_{0.7}K_{0.3}TiO_{3-\delta}$@PC-polyHIPEs is increased to 2.041 $m^2 g^{-1}$, indicating that the large surface of $Sr_{0.7}K_{0.3}TiO_{3-\delta}$ is successfully incorporated into the PC-polyHIPEs.

Figure 5 shows the TG-DTG plot of the pure $Sr_{0.7}K_{0.3}TiO_{3-\delta}$ nanoparticles, PC-polyHIPEs, and the composite $Sr_{0.7}K_{0.3}TiO_{3-\delta}$@PC-polyHIPEs. The weight loss of pure $Sr_{0.7}K_{0.3}TiO_{3-\delta}$ (Figure 5(a)) is very tiny with 0.8 wt.% during the heating process from 20 to 800°C, suggesting that the as-fabricated $Sr_{0.7}K_{0.3}TiO_{3-\delta}$ is extremely

steady. By contrast, the weight loss of PC-polyHIPEs is almost 100% (Figure 5(b)), indicating the total combustion in air. The PC-polyHIPEs exhibits marked mass loss peaks at around 264°C, 369°C, and 455°C, while the composite material $Sr_{0.7}K_{0.3}TiO_{3-\delta}$@PC-polyHIPEs also has significant mass loss at the above-mentioned temperatures. After incorporating $Sr_{0.7}K_{0.3}TiO_{3-\delta}$ into PC-polyHIPEs, the residual weight is 45.4 wt.%, demonstrating $Sr_{1-x}K_xTiO_{3-\delta}$ constitutes 45.4 wt.% of $Sr_{1-x}K_xTiO_{3-\delta}$@PC-polyHIPEs.

### 3.2. The Photocatalytic Property of $Sr_{1-x}K_xTiO_3$@PC-polyHIPEs

3.2.1. The Effect of K-Doping. The catalytic performance of $Sr_{1-x}K_xTiO_{3-\delta}$ ($x = 0~0.5$) under UV light is shown in Figure 6. The catalytic performance of $Sr_{1-x}K_xTiO_{3-\delta}$ ($x = 0.1~0.5$) is better than pure $SrTiO_3$. Moreover, the catalytic activity of $Sr_{1-x}K_xTiO_{3-\delta}$ increases with the addition of potassium till $x = 0.3$. The catalyst $Sr_{0.7}K_{0.3}TiO_{3-\delta}$ was the best, over which the degradation rate of MB reached 42% ($C/C_o = 0.58$) when the UV-irradiation time was 20 min. However, when $x > 0.3$, the photodegradation activity of
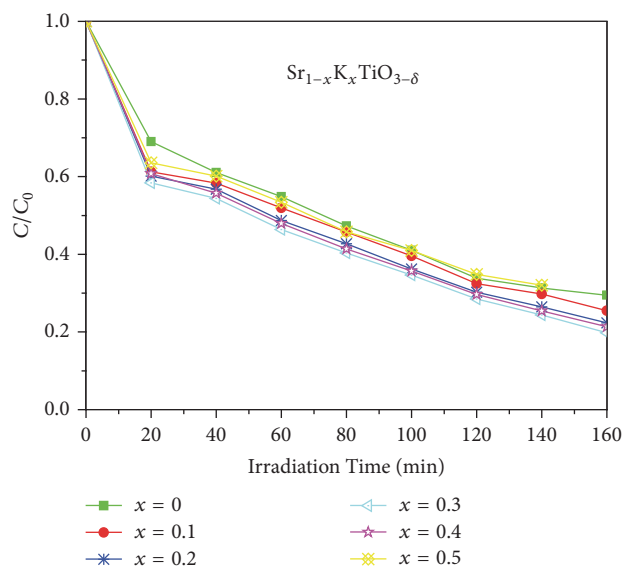
FIGURE 6: Photocatalytic decomposition of MB over $Sr_{1-x}K_xTiO_{3-\delta}$ under UV (365 nm) irradiation.



FIGURE 7: Photocatalytic properties over MB of $Sr_{0.7}K_{0.3}TiO_{3-\delta}$ and $Sr_{0.7}K_{0.3}TiO_{3-\delta}$@PC-polyHIPEs under UV (365 nm) and Vis (450 nm) irradiation.

$Sr_{1-x}K_xTiO_{3-\delta}$ declined. When $x = 0.4, 0.5$, the degradation efficiency of $Sr_{1-x}K_xTiO_{3-\delta}$ for MB was 40% and 36%, respectively, with 20 min UV-irradiation. The photodegradation performance of all the catalysts was significantly improved with the prolongation of the irradiation time. The higher efficiency of $Sr_{1-x}K_xTiO_{3-\delta}$ under UV light can be ascribed to oxygen vacancy generation when potassium doped onto $SrTiO_3$.

According to the results of Figure 6, the optimum K-doping amount is 30% for $Sr_{1-x}K_xTiO_{3-\delta}$ catalysts. Therefore, we choose $Sr_{0.7}K_{0.3}TiO_{3-\delta}$ catalyst and catalyst support PC-polyHIPEs to form new composite $Sr_{0.7}K_{0.3}TiO_{3-\delta}$@PC-polyHIPEs and then study its photodecomposition activity for MB under both UV and visible light. Its photodegradation performance is shown in Figure 7. When PC-polyHIPEs are added, the new photocatalyst $Sr_{0.7}K_{0.3}TiO_{3-\delta}$@PC-polyHIPEs has a very high MB catalytic activity, and the degradation rate can be achieved about 71.9% only under 20 min UV-irradiation. In contrast, $Sr_{0.7}K_{0.3}TiO_{3-\delta}$ has a degradation rate of only 42% when irradiated under UV light for 20 min, showing that the degradation efficiency of $Sr_{0.7}K_{0.3}TiO_{3-\delta}$@PC-polyHIPEs under UV light was increased by 71.4%. After incorporation, the higher efficiency of $Sr_{0.7}K_{0.3}TiO_{3-\delta}$@PC-polyHIPEs under UV light can be ascribed to a better dispersion of $Sr_{0.7}K_{0.3}TiO_{3-\delta}$ onto PC-polyHIPEs, which increases the active sites of catalyst exposed to MB. Some small particles around 10 nm attached inside the pores of PC-polyHIPEs may cause quantum efficiency enhancement [27].

It can be observed from Figure 7 that pure $Sr_{0.7}K_{0.3}TiO_{3-\delta}$ has no photocatalytic activity under visible light, so do PC-polyHIPEs. However, after incorporation, $Sr_{0.7}K_{0.3}TiO_{3-\delta}$@PC-polyHIPEs have excellent catalytic efficiency for MB degradation under visible light. The MB degradation rate can reach 56.5% after visible light irradiation for 20 min,
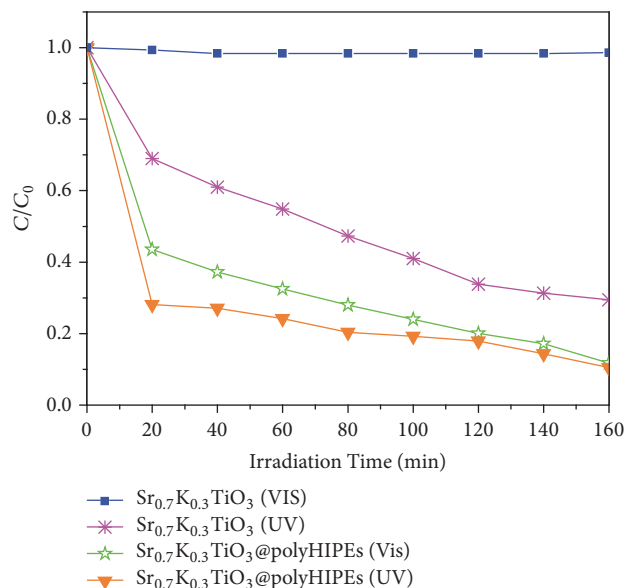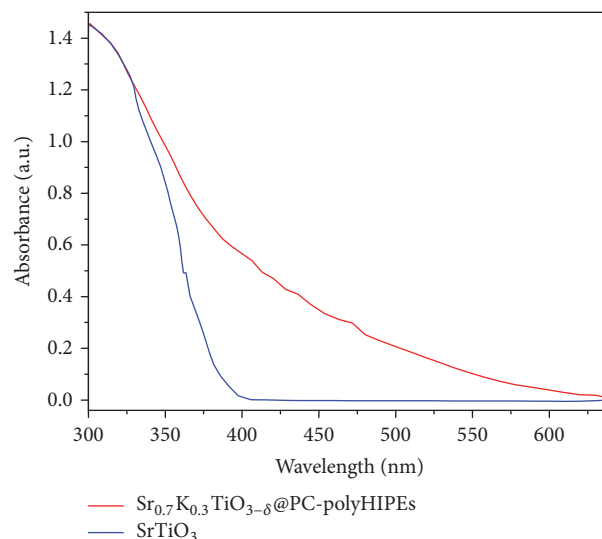


FIGURE 8: UV-Vis DRS spectra of $Sr_{0.7}K_{0.3}TiO_{3-\delta}$@PC-polyHIPEs and neat $SrTiO_3$.

which is impossible for pure $Sr_{0.7}K_{0.3}TiO_{3-\delta}$ alone. When the aqueous suspension containing 50 mg L$^{-1}$ MB and 1.6 g$_{cat.}$ L$^{-1}$ $Sr_{0.7}K_{0.3}TiO_{3-\delta}$@PC-polyHIPEs is exposed to visible light for 160 min at room temperature, 88.3% of MB is decomposed.

To further explore the photocatalytic activity of $Sr_{0.7}K_{0.3}TiO_{3-\delta}$@PC-polyHIPEs under visible light irradiation, UV-Vis DRS spectra of $Sr_{0.7}K_{0.3}TiO_{3-\delta}$@PC-polyHIPEs and neat $SrTiO_3$ were recorded (Figure 8). The light absorption of $SrTiO_3$ ranges from 200 to 400 nm, confirming that it does not absorb visible light. However, the absorption of $Sr_{0.7}K_{0.3}TiO_{3-\delta}$@PC-polyHIPEs ranges from 200 to 640 nm, covering both UV and visible range. Without
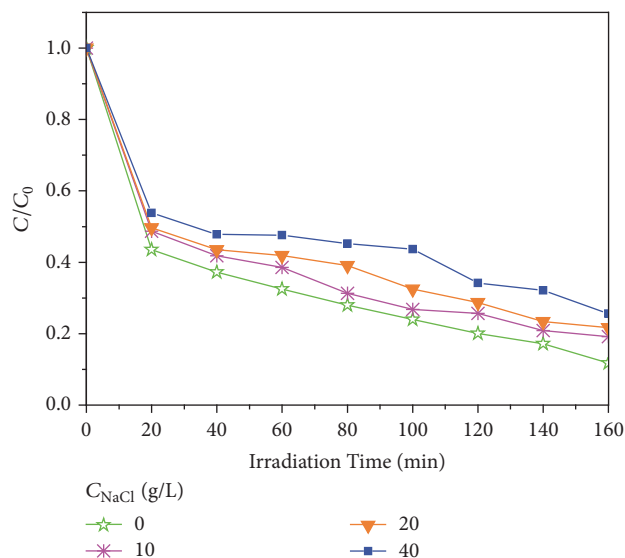
FIGURE 9: Influence of salinity over $Sr_{0.7}K_{0.3}TiO_{3-\delta}$@PC-polyHIPEs for photocatalytic decomposition MB under visible irradiation.



FIGURE 10: Influence of temperature over $Sr_{0.7}K_{0.3}TiO_3$@PC-polyHIPEs for photocatalytic decomposition MB under visible irradiation.

addition of noble metal dopants in the $Sr_{0.7}K_{0.3}TiO_{3-\delta}$ perovskite, the uncommon visible light response of $Sr_{0.7}K_{0.3}TiO_{3-\delta}$@PC-polyHIPEs may be explained by the dye-sensitization or ligand-to-metal charge transfer that occurs between $Sr_{0.7}K_{0.3}TiO_{3-\delta}$ nanoparticles and PC-polyHIPEs [28–30].

*3.2.2. The Effect of Catalyst Concentration.* Since the catalyst concentration has a significant effect on the catalyst activity, the effect of the concentration of $Sr_{0.7}K_{0.3}TiO_{3-\delta}$@PC-polyHIPEs on the activity of photocatalytic degradation of MB is investigated. The concentration of catalyst $Sr_{0.7}K_{0.3}TiO_{3-\delta}$@PC-polyHIPEs is set as 0.4, 0.8, 1.6, and 2.4 $g_{cat.}$ $L^{-1}$, and the light source is visible light. The experimental results show that the degradation efficiency of the catalyst $Sr_{0.7}K_{0.3}TiO_{3-\delta}$@PC-polyHIPEs increases with the increase of the catalyst concentration in the range 0.4~1.6 $g_{cat.}$ $L^{-1}$, as the number of reactive sites increases with rising catalyst concentration [28]. However, when the catalyst concentration reaches 2.4 $g_{cat.}$ $L^{-1}$, the degradation efficiency starts to drop.

*3.2.3. The Effect of Salinity.* Nowadays, a lot of waste water from dyeing has been discharged into the sea. However, the sea water is different from the freshwater resources. It has certain salinity which can affect the activity of catalyst. Therefore, the effect of salinity on the catalytic activity of the composite catalyst is investigated in order to provide a theoretical basis for further industrial applications of the catalyst. Figure 9 shows the photocatalytic degradation properties of $Sr_{0.7}K_{0.3}TiO_{3-\delta}$@PC-polyHIPEs at different salinity ($C_{NaCl}$: 10, 20, 40 $g\,L^{-1}$). It can be seen that the salinity of seawater affects the degradation activity of MB at different levels under visible light compared with the deionized water. When the salinity is increased, the catalytic activity turns low.
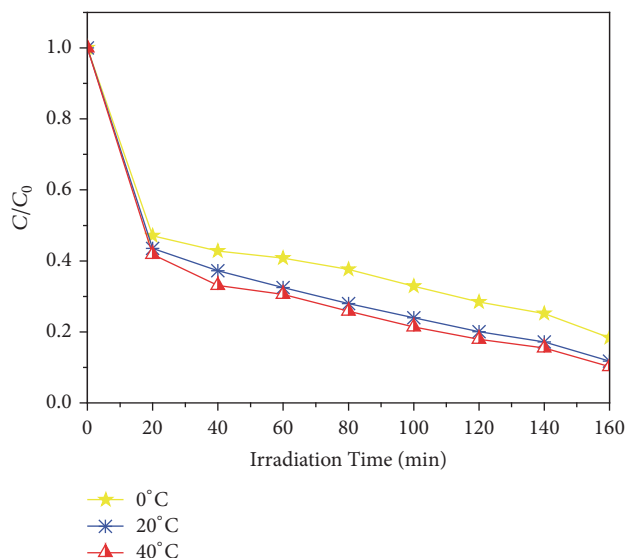
Therefore, the effect order of salinity on the degradation rate of MB over $Sr_{0.7}K_{0.3}TiO_{3-\delta}$@PC-polyHIPEs under visible light from high to low is 40 $g\,L^{-1}$ > 20 $g\,L^{-1}$ > 10 $g\,L^{-1}$. It has been reported that chloride ions may combine with the photocatalyst to affect the excited electron-hole pairing, which has a hindrance effect on the photocatalytic reaction rate [31].

*3.2.4. The Effect of Temperature.* In actual water purification process, the water temperature between summer and winter varies. In order to explore the optimum operating conditions of $Sr_{0.7}K_{0.3}TiO_{3-\delta}$@PC-polyHIPEs, the effect of temperature (0~40°C) on the photocatalytic degradation for MB under visible light is studied and its result is shown in Figure 10. The degradation rates of $Sr_{0.7}K_{0.3}TiO_3$@PC-polyHIPEs are 52.9%, 56.5%, and 59.3% at 0°C, 20°C, and 40°C, respectively, under visible light for 20 min. It can be seen that, with the increase of temperature, the photocatalytic degradation rate is increasing. This is due to the fact that the effective collisions between $Sr_{0.7}K_{0.3}TiO_{3-\delta}$@PC-polyHIPEs and MB are enhanced as the molecules become more active at a higher temperature.

The activation energy ($E$) and reaction order of catalytic reaction are extremely important to studying the process and mechanism of catalytic reactions. Accordingly, the activation energy of $Sr_{0.7}K_{0.3}TiO_{3-\delta}$@PC-polyHIPEs was estimated according to the Ozawa plots. Based on the above results, the activation energy of $Sr_{0.7}K_{0.3}TiO_{3-\delta}$@PC-polyHIPEs for MB decomposition under visible light is calculated to be 12.3 $kJ\,mol^{-1}$. The concentration of MB in the photocatalytic reaction with $Sr_{0.7}K_{0.3}TiO_{3-\delta}$@PC-polyHIPEs under visible light is measured at different time with results shown in Table 2. According to the rate equation using the integral method, if the reaction followed the first-order kinetics, this
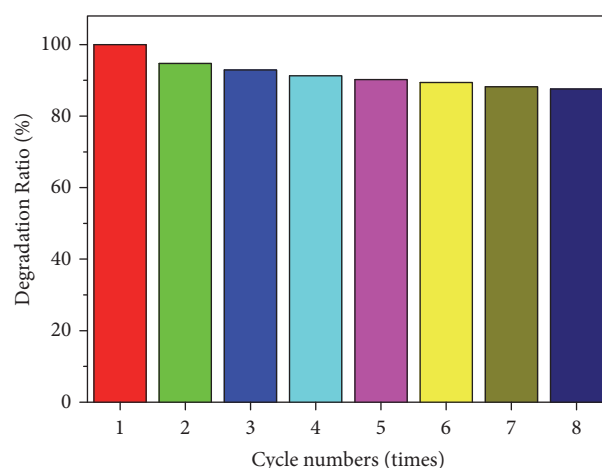
TABLE 2: MB concentration at different time with $Sr_{0.7}K_{0.3}TiO_{3-\delta}$@PC-polyHIPEs under visible light (450 nm).

| Irradiation time $t$, min | MB concentration $C/C_0$, mg/L | $\ln(C/C_0)$ | $1/C$ |
|---|---|---|---|
| 40 | 0.3725 | 0.9875 | 2.2989 |
| 60 | 0.3251 | 1.1239 | 2.6846 |
| 80 | 0.2798 | 1.2737 | 3.0769 |
| 100 | 0.2397 | 1.4284 | 3.5740 |
| 120 | 0.2006 | 1.6064 | 4.1719 |
| 140 | 0.1715 | 1.7632 | 4.9850 |
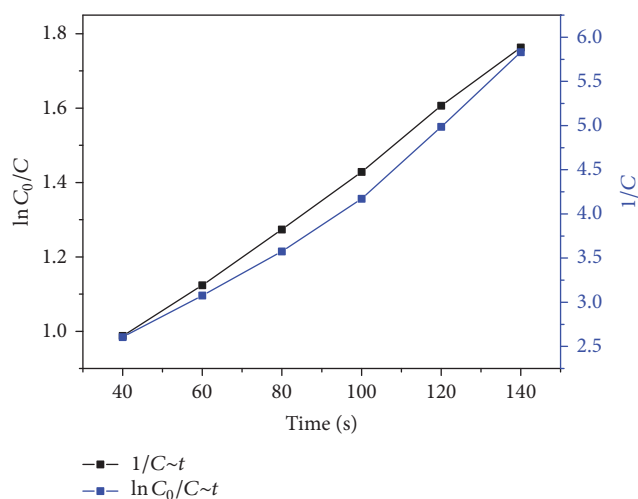


FIGURE 11: The kinetics analysis of $Sr_{0.7}K_{0.3}TiO_{3-\delta}$@PC-polyHIPEs for photocatalytic decomposition MB under visible irradiation.



FIGURE 12: Degradation ratio of MB solutions in the presence of $Sr_{0.7}K_{0.3}TiO_{3-\delta}$@PC-polyHIPEs at eight cycle times.

means that $\ln C_0/C$ versus $t$ (Time) should give a straight line; if the reaction followed the second-order kinetics, this means that $1/C$ versus $t$ should give a straight line. As shown in Figure 11, the $1/C$ versus $t$ gives a straight line; therefore, it can be concluded that the photocatalysis between $Sr_{0.7}K_{0.3}TiO_{3-\delta}$@PC-polyHIPEs and MB under visible light follows the second-order reaction.

*3.2.5. The Effect of Cycle Times.* Figure 12 displays the photocatalytic degradation of MB for 160 min reaction under visible light when $Sr_{0.7}K_{0.3}TiO_{3-\delta}$@PC-polyHIPEs are utilized eight times, yet the photocatalytic activity is well preserved with 87.6% of fresh catalyst degradation ratio even after the eighth cycle. It can be concluded that $Sr_{0.7}K_{0.3}TiO_{3-\delta}$@PC-polyHIPEs have excellent durability and reusability under visible light. Moreover, $Sr_{1-x}K_xTiO_3$@PC-polyHIPEs own many other merits. Firstly, they are flexible and can be separated and collected easily from MB solution. Secondly, the novel material is of low density so it can be floated and easily fixed in water solution, causing high contacting area between catalyst and MB. Thirdly, it is stable either in acid or in base environment and could be suitable for various water conditions. As a kind of low-cost and environment-friendly hybrid material, $Sr_{1-x}K_xTiO_3$@PC-polyHIPEs can

be a promising photocatalyst for water purification under visible light.

## 4. Conclusions

PC-polyHIPEs with large and interconnected pores were fabricated by light-induced polymerization of dopamine in transparent polyHIPEs which were prepared by polymerization within high internal phase emulsions. $Sr_{1-x}K_xTiO_{3-\delta}$ nanoparticles were successfully incorporated and adhered to PC-polyHIPEs to form a novel catalyst compound $Sr_{1-x}K_xTiO_{3-\delta}$@PC-polyHIPEs. The catalyst showed excellent MB decomposition performance under either UV or visible light although $Sr_{1-x}K_xTiO_{3-\delta}$ alone worked only under UV light. When $x = 0.3$, $Sr_{1-x}K_xTiO_{3-\delta}$@PC-polyHIPEs showed the highest photocatalytic performance due to the existence of more oxygen vacancies. When the aqueous suspension with $50 \, mg \, L^{-1}$ MB and $1.6 \, g_{cat.} \, L^{-1}$ $Sr_{0.7}K_{0.3}TiO_{3-\delta}$@PC-polyHIPEs is exposed to visible light for 160 min at room temperature, 88.3% of MB was decomposed. After being used for eight cycles, 87.6% activity of fresh $Sr_{0.7}K_{0.3}TiO_{3-\delta}$@PC-polyHIPEs still remained. The influences of salinity, temperature, and catalyst concentration on the photocatalytic activity were studied. For MB decomposition under visible light, the activation energy

of $Sr_{0.7}K_{0.3}TiO_{3-\delta}$@PC-polyHIPEs was calculated to be $12.3\,kJ\,mol^{-1}$ and the kinetics analysis revealed that the photocatalyst was the second-order reaction. These findings demonstrated that $Sr_{1-x}K_xTiO_{3-\delta}$@PC-polyHIPEs were an effective catalyst in real application for MB degradation.

## Conflicts of Interest

The authors declare that there are no conflicts of interest regarding the publication of this paper.

## Acknowledgments

## Supplementary Materials

Data of photocatalytic decomposition of MB for 160 min under visible light when $Sr_{1-x}K_xTiO_{3-\delta}$@poly-HIPEs were used. (Supplementary Materials)

## References

[1] H. Mohammad, S. H. Hossein, and S. N. Masoud, "Degradation of methylene blue and Rhodamine B as water pollutants via green synthesized $Co_3O_4$/ZnO nanocomposite," *Journal of Molecular Liquids*, vol. 229, pp. 293–299, 2017.

[2] Ü. Geçgel, G. Özcan, and G. Ç. Gürpınar, "Modelling and interpretation of adsorption isotherms," *Journal of Chemistry*, vol. 2017, pp. 1–11, 2017.

[3] H. Park, Y. Park, W. Kim, and W. Choi, "Surface modification of $TiO_2$ photocatalyst for environmental applications," *Journal of Photochemistry and Photobiology C: Photochemistry Reviews*, vol. 15, no. 2, pp. 1–20, 2013.

[4] Y. Li, J. Wang, H. Yao, L. Dang, and Z. Li, "Efficient decomposition of organic compounds and reaction mechanism with BiOI photocatalyst under visible light irradiation," *Journal of Molecular Catalysis A: Chemical*, vol. 334, no. 1-2, pp. 116–122, 2011.

[5] S. Kawasaki, R. Takahashi, K. Akagi et al., "Electronic structure and photoelectrochemical properties of an Ir-doped $SrTiO_3$ photocatalyst," *The Journal of Physical Chemistry C*, vol. 118, no. 35, pp. 20222–20228, 2014.

[6] X. Zhang, K. Huo, L. Hu, Z. Wu, and P. K. Chu, "Synthesis and photocatalytic activity of highly ordered $TiO_2$ and $SrTiO_3$/$TiO_2$ nanotube arrays on Ti substrates," *Journal of the American Ceramic Society*, vol. 93, no. 9, pp. 2771–2778, 2010.

[7] R. Konta, T. Ishii, H. Kato, and A. Kudo, "Photocatalytic activities of noble metal ion doped $SrTiO_3$ under visible light irradiation," *The Journal of Physical Chemistry B*, vol. 108, no. 26, pp. 8992–8995, 2004.

[8] M. Miyauchi, M. Takashio, and H. Tobimatsu, "Photocatalytic activity of $SrTiO_3$ codoped with Nitrogen and lanthanum under visible light illumination," *Langmuir*, vol. 20, no. 1, pp. 232–236, 2004.

[9] R. Niishiro, S. Tanaka, and A. Kudo, "Hydrothermal-synthesized $SrTiO_3$ photocatalyst codoped with rhodium and antimony with visible-light response for sacrificial $H_2$ and $O_2$ evolution and application to overall water splitting," *Applied Catalysis B: Environmental*, vol. 150-151, pp. 187–196, 2014.

[10] Y. Jia, S. Shen, D. Wang et al., "Composite $Sr_2TiO_4$/$SrTiO_3$(La, Cr) heterojunction based photocatalyst for hydrogen production under visible light irradiation," *Journal of Materials Chemistry A*, vol. 1, no. 27, pp. 7905–7912, 2013.

[11] T.-H. Xie, X. Sun, and J. Lin, "Enhanced photocatalytic degradation of RhB driven by visible light-induced MMCT of Ti(IV)-O-Fe(II) formed in Fe-doped $SrTiO_3$," *The Journal of Physical Chemistry C*, vol. 112, no. 26, pp. 9753–9759, 2008.

[12] J. Wang, S. Yin, Q. Zhang, F. Saito, and T. Sato, "Mechanochemical synthesis of $SrTiO_{3-x}F_x$ with high visible light photocatalytic activities for nitrogen monoxide destruction," *Journal of Materials Chemistry*, vol. 13, no. 9, pp. 2348–2352, 2003.

[13] C. W. Lim and I. S. Lee, "Magnetically recyclable nanocatalyst systems for the organic reactions," *Nano Today*, vol. 5, no. 5, pp. 412–434, 2010.

[14] D. Wang, J. H. Ye, T. Kako, and T. Kimura, "Photophysical and photocatalytic properties of $SrTiO_3$ doped with Cr cations on different sites," *The Journal of Physical Chemistry B*, vol. 110, no. 32, pp. 15824–15830, 2006.

[15] A. Desforges, R. Backov, H. Deleuze, and O. Mondain-Monval, "Generation of palladium nanoparticles within macrocellular polymeric supports: Application to heterogeneous catalysis of the Suzuki-Miyaura coupling reaction," *Advanced Functional Materials*, vol. 15, no. 10, pp. 1689–1695, 2005.

[16] F. Su, C. L. Bray, B. Tan, and A. I. Cooper, "Rapid and reversible hydrogen storage in clathrate hydrates using emulsion-templated polymers," *Advanced Materials*, vol. 20, no. 14, pp. 2663–2666, 2008.

[17] C. Féral-Martin, M. Birot, H. Deleuze, A. Desforges, and R. Backov, "Integrative chemistry toward the first spontaneous generation of gold nanoparticles within macrocellular poly-HIPE supports (Au@polyHIPE) and their application to eosin reduction," *Reactive and Functional Polymers*, vol. 67, no. 10, pp. 1072–1082, 2007.

[18] I. Pulko, J. Wall, P. Krajnc, and N. R. Cameron, "Ultra-high surface area functional porous polymers by emulsion templating and hypercrosslinking: Efficient nucleophilic catalyst supports," *Chemistry - A European Journal*, vol. 16, no. 8, pp. 2350–2354, 2010.

[19] Y. Wu, T. Zhang, Z. Xu, and Q. Guo, "High internal phase emulsion (HIPE) xerogels for enhanced oil spill recovery," *Journal of Materials Chemistry A*, vol. 3, no. 5, pp. 1906–1909, 2015.

[20] T. Zhang, Y. Wu, Z. Xu, and Q. Guo, "Hybrid high internal phase emulsion (HIPE) organogels with oil separation properties," *Chemical Communications*, vol. 50, no. 89, pp. 13821–13824, 2014.

[21] T. Zhang, Z. Xu, Y. Wu, and Q. Guo, "Assembled block copolymer stabilized high internal phase emulsion hydrogels for enhancing oil safety," *Industrial & Engineering Chemistry Research*, vol. 55, no. 16, pp. 4499–4505, 2016.

[22] T. Zhang and Q. Guo, "Isorefractive high internal phase emulsion organogels for light induced reactions," *Chemical Communications*, vol. 52, no. 24, pp. 4561–4564, 2016.

[23] T. Zhang and Q. Guo, "Continuous preparation of polyHIPE monoliths from ionomer-stabilized high internal phase emulsions (HIPEs) for efficient recovery of spilled oils," *Chemical Engineering Journal*, vol. 307, pp. 812–819, 2017.

[24] X. Li, G. Sun, Y. Li et al., "Porous $TiO_2$ materials through pickering high-internal phase emulsion templating," *Langmuir*, vol. 30, no. 10, pp. 2676–2683, 2014.

[25] J. Xu, J. Liu, Z. Zhao et al., "Easy synthesis of three-dimensionally ordered macroporous $La_{1-x}K_xCoO_3$ catalysts and their high activities for the catalytic combustion of soot," *Journal of Catalysis*, vol. 282, no. 1, pp. 1–12, 2011.

[26] X. Wei, G. Xu, Z. Ren et al., "Single-crystal-like mesoporous SrTiO3 spheres with enhanced photocatalytic performance," *Journal of the American Ceramic Society*, vol. 93, no. 5, pp. 1297–1305, 2010.

[27] H. Zhang, G. Liu, L. Shi, H. Liu, T. Wang, and J. Ye, "Engineering coordination polymers for photocatalysis," *Nano Energy*, vol. 22, pp. 149–168, 2016.

[28] G. Zhang, G. Kim, and W. Choi, "Visible light driven photocatalysis mediated via ligand-to-metal charge transfer (LMCT): An alternative approach to solar activation of titania," *Energy & Environmental Science*, vol. 7, no. 3, pp. 954–966, 2014.

[29] B. Subash, B. Krishnakumar, M. Swaminathan, and M. Shanthi, "Highly efficient, solar active, and reusable photocatalyst: Zr-loaded Ag-ZnO for reactive red 120 dye degradation with synergistic effect and dye-sensitized mechanism," *Langmuir*, vol. 29, no. 3, pp. 939–949, 2013.

[30] Y. Li, W. Guo, H. Hao et al., "Enhancing photoelectrical performance of dye-sensitized solar cell by doping $SrTiO_3:Sm^{3+}@SiO_2$ core-shell nanoparticles in the photoanode," *Electrochimica Acta*, vol. 173, Article ID 25049, pp. 656–664, 2015.

[31] M. Pelaez, N. T. Nolan, S. C. Pillai et al., "A review on the visible light active titanium dioxide photocatalysts for environmental applications," *Applied Catalysis B: Environmental*, vol. 125, pp. 331–349, 2012.